



Thermal analysis of MgFe-Cl Layered doubled hydroxide (LDH) directly synthesized and produced “via memory effect”

Anna Maria Cardinale¹ · Marco Fortunato¹ · Federico Locardi¹ · Nadia Parodi¹

Received: 26 April 2021 / Accepted: 3 January 2022 / Published online: 24 January 2022
© The Author(s) 2022

Abstract

Layered doubled hydroxides (LDHs) are known to be an interesting class of 2D layered materials, with a wide range of possible composition and a flexible structure suitable for topochemical reactions. Thus, LDHs have been applying in different fields, such as catalysis, energy storage and all the applications in which a high exchange capability (of both cations and anions) is required. For remediation purpose, a MgFe-Cl LDH $[(Mg_{0.66}^{2+}Fe_{0.33}^{3+}(OH)_2)^{0.33+}(Cl_{0.33}^-)^{0.33-}]$ (MFC in the following) could be a promising candidate to capture the toxic CrO_4^{2-} from water, in exchange with the Cl^- in an efficient way. The synthesis of this compound might seem simple, consisting of a coprecipitation reaction, and actually, it is strongly affected by the environmental carbon dioxide able to replace the Cl^- with the more stable CO_3^{2-} . To avoid this problem, LDHs could be also prepared with a rehydration of their calcinated oxide (memory effect). In this work were prepared two samples of MFC: one via coprecipitation (MFC-1 in the following) and one via “memory effect” (MFC-mem in the following). Both the compounds were characterized by means of X-ray powder diffraction (PXRD), Fourier transform infrared spectroscopy (FT-IR) and differential thermal analysis-thermogravimetry (DTA-TG) coupled with evolved gas analysis. The results demonstrated that the synthesis of pure MFC is very difficult, and only a minimum contamination of carbon dioxide led to the formation of the carbonate LDH in a massive way. It was also demonstrated that Mg-Fe LDHs in the presence of carbonate could catalyse the formation of the formic acid (HCOOH) at low temperature (< 300 °C).

Keywords LDHs · Thermal analysis · Memory effect

Introduction

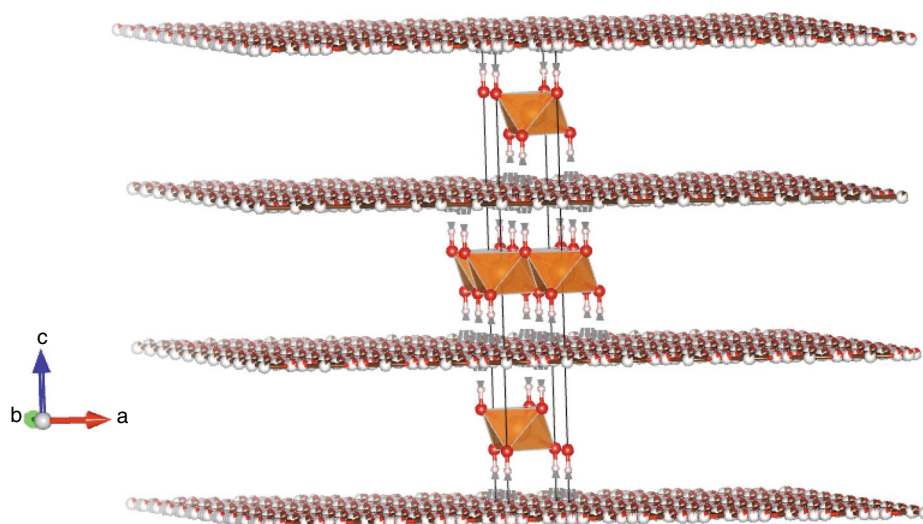
Chromium is one of the most common and toxic pollutants, owing to its bioaccumulation behaviour [1], mobility, solubility [2] and high carcinogenicity [3]. Nowadays, various strategies have been developed to remove Cr (VI) from aqueous solution [4]. But ion exchange method seems to represent one of the best choices, combining both high efficiency and low costs. Until now the main used ion exchanging tools have been ionic-exchange resins that are subject to the pH influence and the degradation while using [5]. To overcome those problems, different solutions have been studied, and LDHs result to be promising materials in this field of application. LDHs general formula is $[M_{1-x}^{2+}N_x^{3+} \cdot (OH)_2]^{x+}(A_n^{n-})^{x-} \cdot mH_2O$,

where M and N are, respectively, a divalent and a trivalent metallic cation, A is an anion with n charge, X is the molar ratio $\frac{N}{N+M}$, and m is a number from 1 to 4. The structure of LDHs can be derived from the structure of *brucite* $Mg(OH)_2$, consisting of layers of Mg^{2+} octahedrally coordinated with six hydroxide anions; in an LDH occurs the replacement of a fraction of the Mg^{2+} ions with a trivalent cation, leading to a positive charge on the surface, which necessitates a balancing anion at the interlayer. These $M^{2+}/N^{3+}(OH)_6$ octahedra form 2D sheets via edge-sharing and may be connected sheet to sheet by hydrogen bridge bonding between the hydroxide groups. As the structure, LDHs similarly to hydrotalcite belong to the space group $R\bar{3}m$ [6], and Fig. 1 shows the typical structure of LDHs compounds. The interlayer region is very flexible and able to host several types of compounds, both anions (strongly bonded), cations and organic molecules. This property explains the interest in these materials as catalysts, anionic sponge [7, 8] and cations adsorber [7–9]. More recently, LDHs are attracting interest in the energy storage systems area, both as supercapacitors and batteries

✉ Marco Fortunato
marco.fortunato@edu.unige.it

¹ Dipartimento di Chimica e Chimica Industriale, Università di Genova, Via Dodecaneso 31, 16146 Genova, Italy

Fig. 1 Ideal schematic structure of an LDH with hydroxide octahedra and its interlayered compounds



materials [10, 11]. The synthesized LDHs crystals are usually very small (around 30 Å), and the texture, especially if prepared hydrothermally, is nanostructured flower-like shaped [12]. MgFe–Cl LDH seems to represent a valid material to replace the toxic CrO_4^{2-} anion in water with the Cl^- . The main problem during the synthesis of MFC is the presence of carbon dioxide (almost unavoidable even if working in inert atmosphere) that could lead to the undesirable formation of the carbonate-LDH, unable to exchange anions. (CO_3^{2-} is very stable in the structure.) In this work, two different samples of MFC were synthesized, following two different synthesis pathways: coprecipitation and reformation via “memory effect”. The aim of this work is to underline the main differences between the two ways of synthesis, the characteristics of the so obtained compounds and which synthesis routine lead to a higher quantity of pure chlorinated LDH.

Experimental procedure

For the synthesis, all the reactants used are supplied by Sigma-Aldrich (St. Louis, Missouri, USA) with technical purity grade.

Two samples of MgFe–Cl LDH were synthesized: the first, with a simple coprecipitation method following the pathway proposed by Wu et al. [13] (from now MFC-1) and the second (from now MFC-mem), starting from calcinated MFC-1 through reformation in a NaCl aqueous solution.

MFC-1 synthesis

In a balloon, under continuous Ar flux (3L min^{-1}), 250 mmol of MgCl_2 and 125 mmol of $\text{FeCl}_3 \cdot 6\text{H}_2\text{O}$ were dissolved in 250 mL of deionized water, and the pH was adjusted to 12.6 with a solution of NaOH dropwise leading to the formation

of a colloidal mixture of metal hydroxides. The so-obtained precipitate with his parent solution was closed under Ar atmosphere, in a dark bottle, (to avoid photocatalyzed side reactions) in an oven at 85 °C for 2 h leading to the recrystallization of the solid and the formation of the LDH structure. The obtained compound was washed with deionized water and separated by centrifugation (2 min, 7500 rpm) several times till the pH of the upper liquid reached the value of 7. The LDH was dried in oven overnight at 60 °C and then grinded to a grain size lower than 125 μm.

All the distilled water used was boiled and stored in a bottle with Ar atmosphere to eliminate the presence of carbon dioxide and carbonates.

MFC-mem synthesis

A portion of the previously obtained MFC-1 was treated for 4 h at 400 °C to eliminate the interlayer compounds obtaining a calcinated compound (MFC-calc) that is a mixture of metal oxides not jet crystalized. MFC-calc was treated with a 1 M Cl^- aqueous solution, prepared with boiled water, under Ar atmosphere in a mixing machine to reform the LDH structure with the Cl^- anion at the interlayer. After the mixing, the solid was filtered and washed with deionized water and dried at 60 °C overnight and then grinded similarly to MFC-1.

All the samples were characterized by means of X-ray powder diffraction (PXRD), Fourier transform infrared spectroscopy (FT-IR), differential thermal analysis-thermogravimetry (DTA-TG) coupled with gas chromatography-mass spectrometry (GC–MS) and elemental analysis. PXRD patterns were collected using X’Pert MPD (Philips, Almelo, Netherland) X-ray powder diffractometers equipped with a Cu anticathode ($K\alpha_{1\text{Cu}} = 1.5406 \text{ \AA}$). The indexing of the obtained diffraction data was performed in comparison with

the literature [14], and the lattice parameters of the phases were calculated using the program LATCON [15]. FT-IR spectra were collected using a Spectrum 65 FT-IR Spectrometer (PerkinElmer, Waltham, MA, USA) equipped with a KBr beam-splitter and a DTGS detector by using an ATR accessory with a diamond crystal; the spectra were recorded from 4000 to 600 cm^{-1} . DTA/TG-GC-MS analyses were performed using a LabsysEvo 1600-Setaram coupled with a TraceGC ultra and DSQ I (ThermoFisher); about 20 mg of sample was placed in an open alumina crucible and heating from 30 °C to 1250 °C, at 10 °C/min under a He atmosphere (60 mL min^{-1}). The sampling of the evolved gases was carried out through a dedicated autosampler (Automation), set at 280 °C, that was collected and injected every minute into the GC. The GC was set in an isothermal mode at 110 °C with the following parameters: inlet temperature 280 °C; carrier gas He 1.2 mL min^{-1} ; split ratio 1:10; split flow 12 mL min^{-1} ; column Mega-5 (5% phenyl-95% methylpolysiloxane; length 30 m; internal diameter: 0.25 mm; and film thickness: 0.25 μm). The gas analysis was performed using a MS-quadrupole operating in the EI mode (70 eV); ion source at 250 °C; transfer line at 280 °C; and mass interval (m/z range) 10–200. The mass spectra identification was performed using the NIST Mass Spectral Search Program for the NIST/EPA/NIH Mass Spectral Library Version 2.2. The elemental analysis was performed by an EA1110 Elemental Analyser (Fison-Instruments, Milan, Italy); all compounds were analysed for C, H, N and S, and the analytical results were within $\pm 0.4\%$ of the theoretical values.

Results and discussion

PXRD

As shown in Fig. 2, the diffraction pattern of MFC-1 and MFC-mem is similar, showing the typical symmetric (003) (006) (110) (113) and asymmetric (009) (015) (018) reflections, as reported in the literature for the MgFe-LDH [16]. From this data, the cell parameters

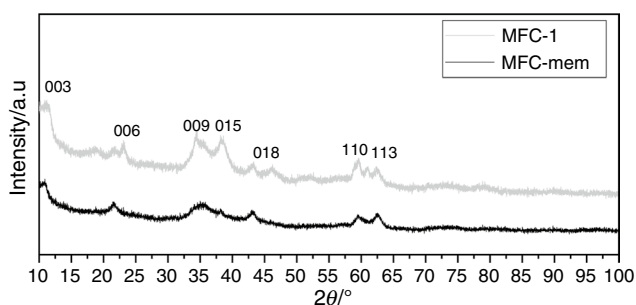


Fig. 2 XRPD patterns of MFC-1 and MFC-mem

have been calculated giving the following results: MFC-1 $a = 0.3122(3)$ nm, $c = 2.3042(48)$ nm, $V_{\text{cell}} = 0.1945(5)$ nm^3 and MFC-mem $a = 0.3103(3)$ nm, $c = 2.4641(60)$ nm, $V_{\text{cell}} = 0.2055(6)$ nm^3 . In MFC-1 diffraction pattern, there is a peak at 18° attributable to an excess of $\text{Mg}(\text{OH})_2$ not reacted. Comparing the two XRD patterns, it can be observed that the plot related to the MFC-mem appears shifted towards lower angles, indicating a higher d value. The value of $d(003)$ approximately represents the space which includes one Mg/Fe octahedra layer and the interlayer region (basal spacing) [6]. The calculated d values are $d_{(003)}^{\text{MFC-1}} = 0.7634$ nm and $d_{(003)}^{\text{MFC-mem}} = 0.8160$ nm, evidencing a difference of 6.5%. The hydroxide layer thickness is approximately estimated in 0.24 nm [17], so the interlayer regions thickness can be estimated 0.52 nm and 0.58 nm, respectively. The difference in the interlayer size for the two compounds underlines the presence of a different ratio of carbonate and chloride anions in the interlayer region. Moreover, the broadness of the peaks clearly indicates the nanometric size of the crystallites. After the thermal analysis, *i.e.*, after a thermal treatment at 1250 °C in inert atmosphere, the structure of both MFC-1 and MFC-mem changes from a hexagonal structure in a cubical spinel-like one (Fig. 3), attributable to the transformation of the LDH in magnesioferrite (MgFe_2O_4) [18]. The difference in the position of the peaks persists but is lower than in the pristine compounds. Yet, the diffraction peaks become sharp indicating a natural increase in the crystallite sizes. Furthermore, the cell parameters of the two oxides are, respectively, MFC-1(after TG) $a = 0.8369(9)$ nm and MFC-mem (after TG) $a = 0.8388(4)$ nm.

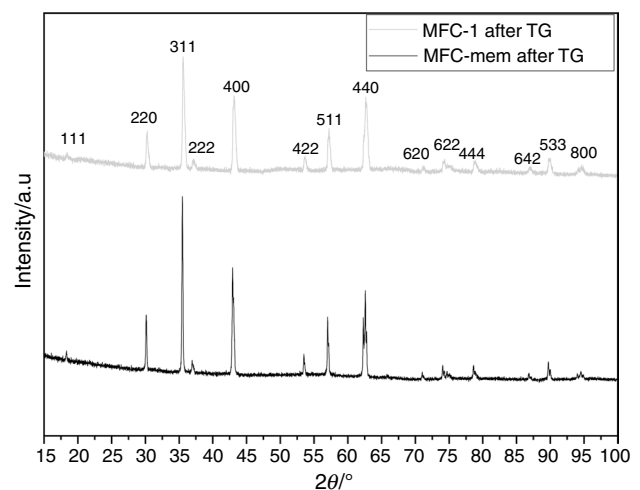


Fig. 3 XRPD patterns of MFC-1 and MFC-mem after the thermal analysis

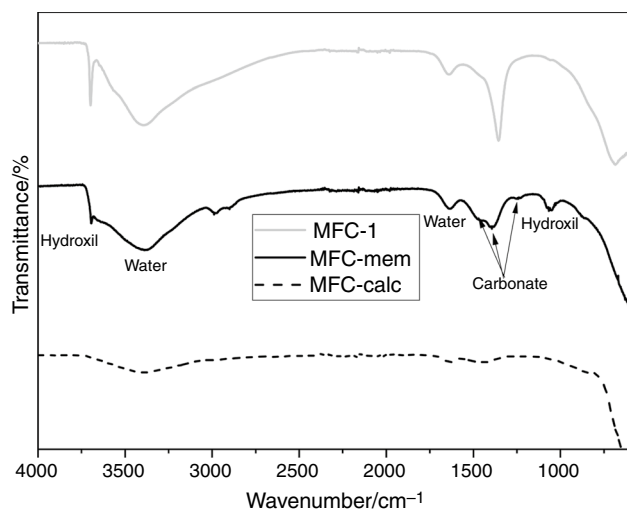


Fig. 4 FT-IR spectra of MFC-1, MFC-mem and MFC-calc (calculated at 400 °C)

FT-IR

Figure 4 shows the FT-IR spectra for the MFC-1 (before and after the heating process at 400 °C) and MFC-mem compounds. By comparing the three spectra, we obtain that the carbonate anion in these structures exists in two different sites and consequently differently bonded. Carbonate anion is hosted in the interlayer and directly bonded with a transition metal in the lattice (in this case Fe). The spectrum related to MFC-1 shows the higher amount of the interlayered carbonate, and the absorption band due to the vibrational modes of the very symmetric interlayer carbonate results in a single large band at 1355 cm⁻¹ with a small shoulder at 1470 cm⁻¹. In MFC-calc, all the interlayered compounds were eliminated, and the spectrum shows only an almost negligible signal in the zone of the carbonates. Indeed at 180 °C, the interlayer carbonate reacts with part of the crystal water according to the reaction (Eq. 1) proposed by Eiji et al. [19]; the only carbonate signal in this spectrum is due to the anion in coordination with iron. In MFC-mem, the signal of the carbonate is split in 4 smaller peaks at about 1530–1500–1400–1300 cm⁻¹ due to the contribution of both interlayered (less intense than in MFC-1) and directly bonded anion.



DTA/TG-GC-MS

As shown in Fig. 5a, both MFC-1 and MFC-mem lose mass through four main steps. The first two from 100 °C

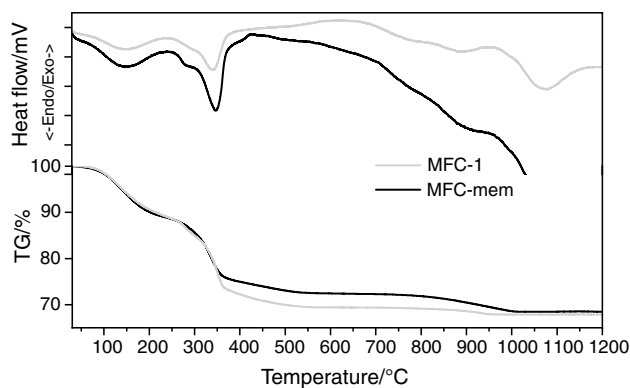
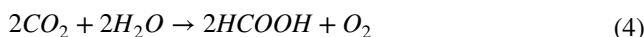


Fig. 5 TG-DTA paths of MFC-1 and MFC-mem **a** TG curve of MFC-1 and MFC-mem. **b** DTA curve of MFC-1 and MFC-mem

to ~330 °C are attributable to the evolution of water and CO₂ as confirmed by the GC-MS trace (Fig. 6). The first mass decreasing (starting from about 100 °C) follows the reaction reported in Eq. 1, while the second (from 280 °C) is due to the dehydration of hydroxides and calcination of some directly bonded carbonate as reported, respectively, in Eq. 2 and Eq. 3.

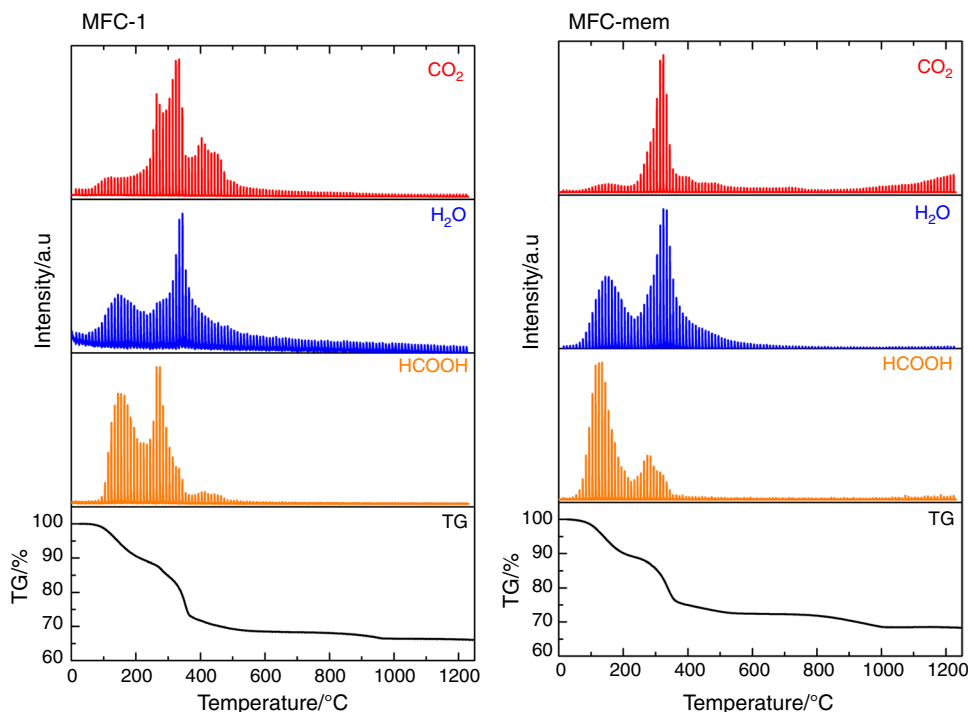


In MFC-1, the two processes end at 350 °C leading to a mass decrease of 23.0%, whereas in MFC-mem it ends at 340 °C with a 20.3% mass loss; at this point the LDH structure is completely degraded in both samples. The end point of the thermal effects for both the analysis was determined from the stronger endothermic peaks in the DTA curves, as shown in Fig. 5b. Moving towards higher temperature (from ~400 °C), another mass loss, higher for MFC-1 than for MFC-mem, and related again to carbon dioxide, occurs (Fig. 6). The mass loss related to the temperature range between 400 °C and 800 °C is of a 4% higher for MFC-1 with respect to MFC-mem. Interestingly, during the decomposition at T < 400 °C a massive formation of formic acid (HCOOH) was also detected for both the compounds. This acid was not used during the synthesis of the LDH, so it has to be formed during the thermal analysis by reactions between CO₂ and water, probably catalysed by the LDH structure itself following the reaction suggested in Eq. 4.



The study of the mechanism and the kinetic of the previous reactions definitely deserve interest and will be investigated in further works. The fourth step at a temperature higher than 900 °C leads to an additional mass loss, evolving something that is not revealed by the

Fig. 6 TG-MS trace of water, carbon dioxide and formic acid of MFC-1 and MFC-mem



GC-MS device, probably some chlorinated salt volatile at that temperature. This last step is larger in MFC-mem than in MFC-1 and leads to a final total mass loss of the 32% in both samples. During the whole thermal analysis, for both LDHs, it does not reveal any chlorinated compound but only CO₂, water and formic acid. The presence of chlorine has to be researched in the last mass step with the evolution of probable volatile salt undetectable by the GC-MS. This could be in accordance with the higher step in the last mass loss of the MFC-mem.

Elemental analysis

The elemental analysis on the samples MFC-1 and MFC-mem provides the mass percentage of C, H, N and S; in both cases, the amount of the last two elements was 0%.

In MFC-1, 1.89% of C and 2.65% of H that means 6.94% of CO₂ and 23.85% of H₂O are present.

In MFC-mem, 1.27% of C and 2.33% of H corresponding to 4.66% of CO₂ and 20.97% of H₂O are present.

Those results fit perfectly with the TGA ones. In MFC-1, the sum of the carbon dioxide and water contributions correspond to a value of 30.79 mass%, while in MFC-mem this value is 25.63 mass%. The 5 mass% difference is due to the last mass loss (Fig. 5) in the TGA results, and it is attributable to the evolution of chlorinated salts.

Conclusions

All the analysis leads to the conclusion that both the synthesis pathways of the LDH, direct coprecipitation and the memory effect reforming, are not suitable to obtain a pure chlorinated LDH. The synthesis method based on the memory effect seems to be more performing than the simple coprecipitation, but leads only to a low percentage of the desired compound. Probably pure MFC could be synthesized only in very controlled condition such as in a “glove-box”, making this method a little more laborious and expensive. The GC-MS analysis during the DTA/TG allowed us to state that the Mg-Fe LDH might be a potential catalyst for the formation of the formic acid (HCOOH) at low temperature (when the oxides are not yet formed).

Open Access This article is licensed under a Creative Commons Attribution 4.0 International License, which permits use, sharing, adaptation, distribution and reproduction in any medium or format, as long as you give appropriate credit to the original author(s) and the source, provide a link to the Creative Commons licence, and indicate if changes were made. The images or other third party material in this article are included in the article's Creative Commons licence, unless indicated otherwise in a credit line to the material. If material is not included in the article's Creative Commons licence and your intended use is not permitted by statutory regulation or exceeds the permitted use, you will need to obtain permission directly from the copyright holder. To view a copy of this licence, visit <http://creativecommons.org/licenses/by/4.0/>.

References

- Ugulu I, Khan ZI, Safdar H, Ahmad K, Bashir H. Chromium Bioaccumulation by Plants and Grazing Livestock as Affected by the Application of Sewage Irrigation Water: Implications to the Food Chain and Health Risk. *Int J Environ Res*. 2021. <https://doi.org/10.1007/s41742-021-00311-7>.
- Standeven AM, Wetterhahn KE. Chromium(VI) Toxicity: Uptake, Reduction, and DNA Damage. *J Am Coll Toxicol*. 1989; <https://doi.org/10.3109%2F10915818909009118>
- Vaiopoulou E, Gikas P. Regulations for chromium emissions to the aquatic environment in Europe and elsewhere. *Chemosphere*. 2020. <https://doi.org/10.1016/j.chemosphere.2020.126876>.
- Karimi-Maleh H, Orooji Y, Ayati A, Qanbari S, Tanhaei B, Karimi F, Alizadeh M, Rouhi J, Fu L, Sillanpää M. Recent advances in removal techniques of Cr(VI) toxic ion from aqueous solution: A comprehensive review. *J Mol Liq*. 2020. <https://doi.org/10.1016/j.molliq.2020.115062>.
- Marcu C, Balla A, Balázs JZS, Lar C. Adsorption Isotherms and Thermodynamics for Chromium (VI) Using an Anion Exchange Resin. *Anal Lett*. 2020. <https://doi.org/10.1080/00032719.2020.1825464>.
- Cavani F, Trifirò F, Vaccari A. Hydrotalcite-type anionic clays: Preparation, properties and applications. *Cat Today*. 1991. [https://doi.org/10.1016/0920-5861\(91\)80068-K](https://doi.org/10.1016/0920-5861(91)80068-K).
- Li F, Duan X. Applications of Layered Double Hydroxides. *Struct Bond*. 2005. https://doi.org/10.1007/430_007.
- Sayed MR, Abukhadra MR, Ahmed SA, Shaban M, Javed U, Betiha MA, Shim JJ, Rabie AM. Synthesis of advanced MgAl-LDH based geopolymer as a potential catalyst in the conversion of waste sunflower oil into biodiesel: Response surface studies. *Fuel*. 2020. <https://doi.org/10.1016/j.fuel.2020.118865>.
- Cardinale AM, Carbone C, Consani S, Fortunato M, Parodi N. Layered double hydroxides for remediation of industrial wastewater from a galvanic plant. *Curr Comput-Aided Drug Des*. 2020. <https://doi.org/10.3390/cryst10060443>.
- Liu H, Yu T, Su D, Tang Z, Zhang J, Liu Y, Yuan A, Kong Q. Ultrathin Ni–Al layered double hydroxide nanosheets with enhanced supercapacitor performance. *Ceram Int*. 2017. <https://doi.org/10.1016/j.ceramint.2017.07.207>.
- Shi L, Chen Y, He R, Chen X, Song H. Graphene-wrapped CoNi-layered double hydroxide microspheres as a new anode material for lithium-ion batteries. *Phys Chem Chem Phys*. 2018. <https://doi.org/10.1039/c8cp01681j>.
- Rao MM, Reddy BR, Jayalakshmi M, Jaya VS, Sridhar B. Hydrothermal synthesis of Mg–Al hydrotalcites by urea hydrolysis. *Mat Res Bull*. 2005; <https://doi.org/10.1016/j.materresbull.2004.10.007>
- Wu J, Lin J, Zhan Y. Interception of phosphorus release from sediments using Mg/Fe-based layered double hydroxide (MF-LDH) and MF-LDH coated magnetite as geo-engineering tools. *Sci Tot Environ*. 2020. <https://doi.org/10.1016/j.scitotenv.2020.139749>.
- Villarkas P, Cenzual K. Pearson's Crystal Data- Crystal Structure Database for Inorganic Compounds, Release 2017/18, ASM international, Materials Park, Ohio, USA.
- King G, Schwarzenbach LD., Xtal3.7 system, in Hall SR, du Boilay DJ, Olthof-Hazekamp R, editors. *Crawley: University of Western*; 2000
- Kang D, Yu X, Tong S, Ge M, Zuo J, Cao C, Song W. Performance and mechanism of Mg/Fe layered double hydroxides for fluoride and arsenate removal from aqueous solution. *Chem Eng J*. 2013. <https://doi.org/10.1016/j.cej.2013.05.041>.
- Liao L, Zhao N, Xia Z. Hydrothermal synthesis of Mg-Al layered double hydroxides (LDHs) from natural brucite and Al(OH)₃. *Mat Res Bull*. 2012. <https://doi.org/10.1016/j.materresbull.2012.07.007>.
- Amer MA, Meaz T, Yehia M, Attalah SS, Fakhry F. Characterization, structural and magnetic properties of the as-prepared Mg-substituted Cu-nanoferrites. *J Alloy Compd*. 2015. <https://doi.org/10.1016/j.jallcom.2015.01.161>.
- Kanezaki E. Thermal behaviour of the hydrotalcite-like layered structure of Mg and Al-layered double hydroxides with interlayer carbonate by means of in situ powder HTXRD and DTA/TG. *Solid State Ion*. 1999. <https://doi.org/10.1016/S0167>.

Publisher's Note Springer Nature remains neutral with regard to jurisdictional claims in published maps and institutional affiliations.